

Light Emitting Diode Irradiation Can Control the Morphology and Optical Properties of Silver Nanoparticles

Kevin G. Stamplecoskie and Juan C. Scaiano*

Centre for Catalysis Research and Innovation, Department of Chemistry, University of Ottawa, 10 Marie Curie, Ottawa, Ontario K1N 6N5, Canada

Received November 26, 2009; E-mail: tito@photo.chem.uottawa.ca

A facile method for the preparation of silver nanoparticles (AgNPs) of various sizes and morphologies, including dodecahedra, nanorods, and nanoplates, has been discovered. We describe a photochemical synthesis of citrate mildly stabilized spherical AgNPs that can in turn be used to prepare multiple nanostructures with predictable and controllable size and morphology through irradiation with inexpensive narrow band LEDs. We also describe a common mechanism for the formation of the various types of AgNP. The changes in morphology also result in dramatic spectroscopic changes, as illustrated in Figure 1.

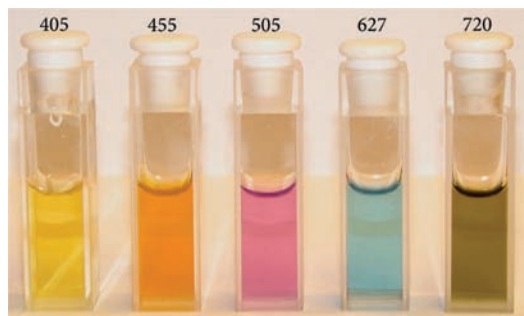
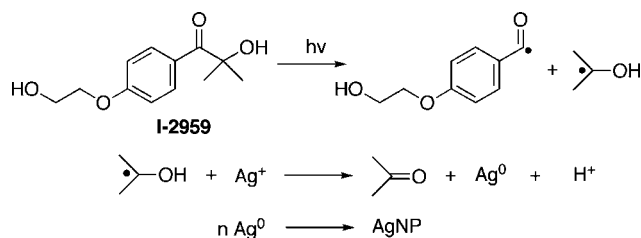


Figure 1. Image of the various colloidal solutions produced under the corresponding LED irradiation at the wavelength indicated (in nm) at the top of each cuvette. All solutions are derived from the same seed stock solution and only differ on the wavelength and exposure time (*vide infra*).

Silver nanostructures are valuable materials for surface enhanced Raman scattering (SERS), optoelectronics, surface-enhanced fluorescence, sensing using surface plasmon resonance (SPR) spectroscopy, catalysis, and numerous biomedical applications; this has led to extensive research into silver nanomaterials,^{1,2} since the properties and applicability of the AgNPs are drastically influenced by their size, shape, and optical properties. For example, in the case of SERS morphology greatly influences the enhancement observed.^{3,4}

There are many thermal methods for the synthesis as well as to control the shape of AgNPs.¹ Thermal synthesis of the various shapes (plates, dodecahedra, rods, etc.) is usually fast but gives a broad particle polydispersity and requires strong reducing agents and frequently high temperatures.¹⁻⁵ Nevertheless, thermal methods are available for producing silver nanowires, nanorods, nanobeams, nanobars and nanorice, nanocubes, rod needles and plate belts, dodecahedra, bipyramids, nanoplates and nanoprisms, and other complex structures.⁵⁻⁷ Photochemical methods have also been developed for the synthesis of spherical nanoparticles,⁸ dodecahedra,⁹ and nanoprisms.^{3,10} The advantages of photochemical methods are that they have excellent spatial and temporal control, avoid the use of harmful strong reducing agents, and are frequently room

Scheme 1. Synthesis of AgNP Seeds



temperature procedures. Further, reducing agents and other materials used in thermal synthesis can leave chemical debris on the nanostructure surface; in contrast, light is simply turned off at the end of the synthesis. Current photochemical synthesis of nanospheres shows little control over particle size, unless one uses a variety of techniques to produce the colloids. The synthesis of plates and dodecahedra require prolonged irradiation and also strong reducing agents such as citrate or NaBH₄ to form the initial AgNP, followed by modification with a variety of stabilizing agents such as L-arginine and poly(vinyl pyrrolidone) (PVP).

For us it was critical to obtain small AgNP seeds, since the shape control methods reported here all lead to particle growth; further to prepare dodecahedra, small seeds are indispensable. An aqueous solution of I-2959 and AgNO₃ containing citrate was photolyzed with UVA light. The citrate arrests the growth of the particles at ~3 nm. Further details are given in the Supporting Information (SI). See Scheme 1 and Figure 2.

Size control over spherical AgNPs was achieved by irradiating a solution of AgNP seeds in our LED apparatus with four LEDs with λ_{max} 405 nm; spectral changes in the UV-vis region are shown in Figure 3. Upon 405 nm excitation the AgNP colloids show a λ_{max} shift from 395 to 416 nm. The maximum at ~395 nm is due

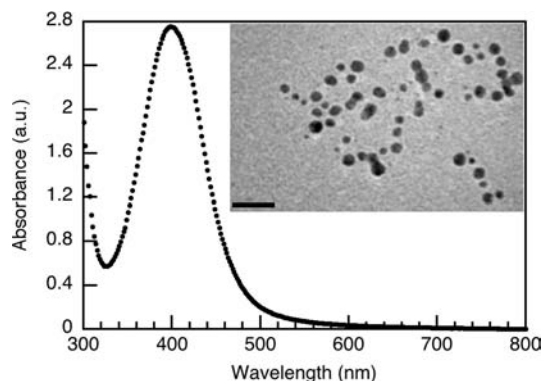


Figure 2. A representative UV/vis absorption spectrum of a 0.2 mM Ag⁺ solution after UVA irradiation and a TEM image of the AgNP seeds with a scale bar of 20 nm.

to the dipolar plasmon absorption of 3.3 ± 0.4 nm AgNP colloids (our seeds), and according to Mie theory the increasing contribution of higher order plasmon modes results in a red shift in their absorption.^{11,12} Figure 3 shows the change in average particle size against irradiation time as determined by SEM (see Figure S2 in the SI). The change in particle size and the red shift in the plasmon absorption with increasing irradiation are a consequence of 405 nm excitation. The process begins as a rapid change in size (see first minute) attributed to the initially high concentration of small reactive AgNP seeds that combine to make larger particles; the rate of growth decreases as the particles coalesce at longer times.

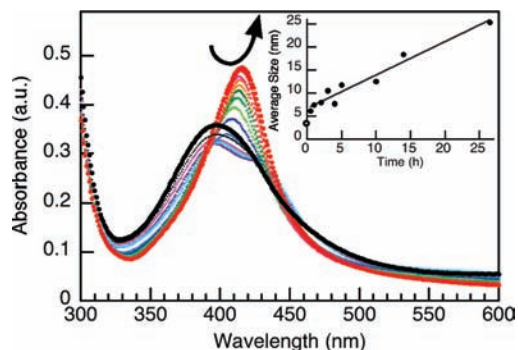


Figure 3. UV/vis spectral change upon 405 nm irradiation (initial in black, final in red) and (inset) change in particle size (determined by SEM) against irradiation time. The line in the plot is simply a visual aid.

Irradiation of AgNP seeds with 455 nm LED causes the spectral changes shown in Figure 4. The end spectrum after irradiation shows a principal absorption at ~ 480 nm due to the in-plane dipole and weaker bands at 400 and 340 nm due to the in-plane quadrupole and the out-of-plane quadrupole plasmon modes, respectively.¹³ The SEM and TEM images of the resultant Ag nanoparticles show complete conversion of seeds to dodecahedra with a narrow polydispersity. For SEM images, see SI.

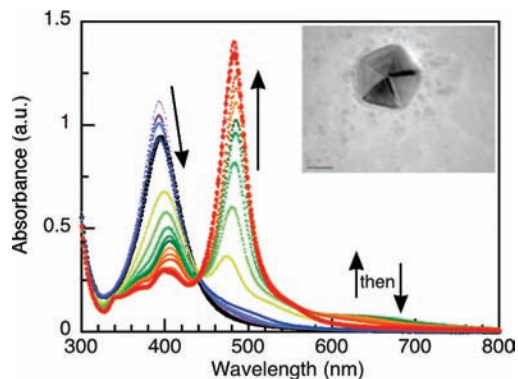


Figure 4. UV/vis spectral change during 455 nm LED excitation (initial in black, final in red); note that at ~ 650 nm the maximum absorbance increases and then decreases at intermediate times (green) during conversion. The inset shows TEM image for a representative particle (size bar = 20 nm).

The irradiation of AgNP seeds with 627 nm light led to the spectral changes of Figure 5, corresponding to the conversion of small spherical seeds to platelets. Figure 5 also shows a representative image of the AgNPs formed that have a large distribution of nanoplates. The new absorption bands in the UV/vis spectrum at 690 and 331 nm are due to the longitudinal and transversal plasmon mode absorptions respectively.³ The same conversion to Ag nanoplates can also be obtained using 590 nm LED irradiation (see SI).

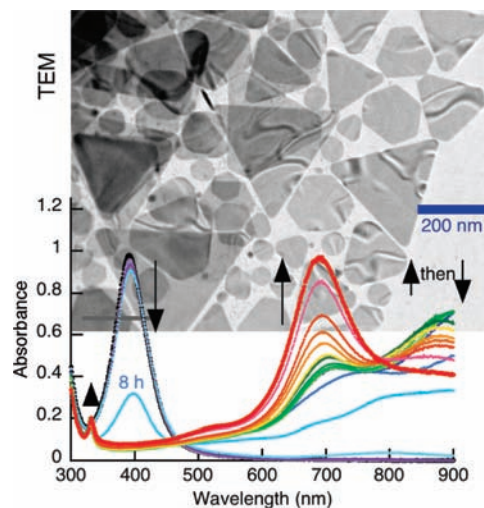


Figure 5. UV/vis spectral change and TEM image (background) during 627 nm LED excitation of AgNP seeds with ~ 900 nm absorption increase and then decrease during the overall conversion.

The spectral change upon 720 nm excitation is shown in Figure 6 (SEM included in Supporting Information). Again, there is a decrease in the dipolar absorption at ~ 395 nm and a subsequent increase in absorbance at 800 nm attributed to the longitudinal plasmon mode of Ag nanorods. While the reproducibility of the synthesis of Ag nanorods proved difficult, the spectroscopic change seen in Figure 6 was always observed for 720 nm irradiation whether the final absorbing species was plates or rods. Figure 6 also includes the image for an exceptionally long rod (70 nm \times 730 nm); most rods had an aspect ratio of 2 or 3.

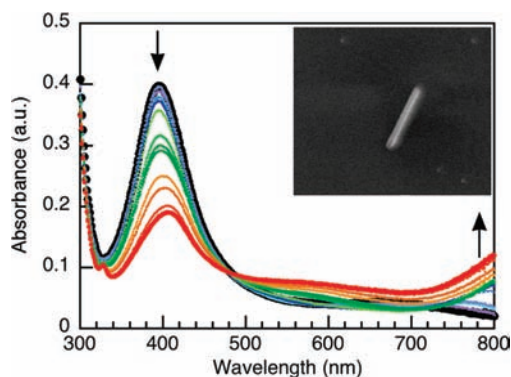
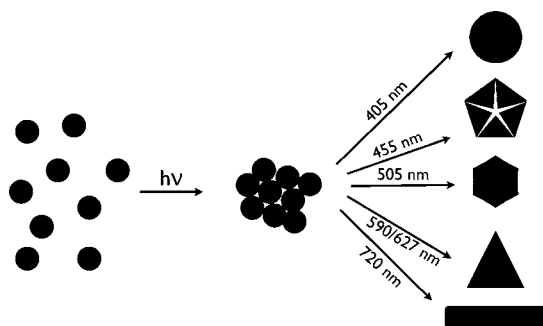


Figure 6. UV/vis spectral change during 720 nm LED irradiation as well as an exceptionally large aspect ratio nanorod (inset).

Upon inspection of the UV/vis absorption spectra of seeds during LED photoconversion to other sizes and morphologies two observations are striking. First, in all cases the major absorption at ~ 395 nm due to the well-known dipolar absorption of citrate-stabilized spherical AgNPs decreases as the absorption band of the final nanostructures increases; e.g., under 627 nm LED irradiation, the dipolar absorption decreases while the longitudinal absorption for platelets at ~ 690 nm increases. Similarly, for dodecahedra and rods the in-plane dipole and longitudinal plasmon modes increase upon 455 and 720 nm irradiation, respectively. In all cases there is also a broad absorption at long wavelengths that increases and then subsequently decreases as the initial seeds are consumed. This long wavelength transient absorption is attributed to aggregates that form during the photoconversion to other shapes, as described by the aggregation/coalescence mechanism of Scheme 2.

Scheme 2. Aggregation/Coalescence Mechanism of Transformation of AgNP Seeds



When metal nanoparticles, especially AgNPs, are excited by light there is a corresponding electromagnetic (EM) field induced surrounding the excited particles that is one of the major mechanisms in SERS enhancement by metal nanoparticles.⁷ In fact the resultant EM field in the vicinity of AgNP is extremely high in comparison with other metals, and it is likely that this is why photoconversion of metal NPs to shapes like plates is dominated by Ag in the literature and why the mechanism proposed here works so well for Ag. This EM field has been shown to cause aggregation and further increase the SERS intensity,¹⁴ and it is this EM field that is used here to cause the transient aggregation of AgNP seeds resulting in the broad absorption characteristic of these aggregates.^{11,15} In all cases the aggregates that form absorb light and the light is efficiently converted to thermal energy that causes coalescence, but if the process was only thermal, then the high energy 410 nm photons should have enough energy to form the most stable dodecahedra but growth to larger spheres is observed instead. It is presumed that O₂ plays an important role in the initial stages of formation of anisotropic seeds as described by Maillard et al.¹⁶ However, in the work by Maillard et al. it is briefly stated that the synthesis of Ag nanoplates becomes nonlinear at high light intensity, which we attribute to the contribution of the aggregation/coalescence mechanism described here that becomes more important under high light intensity (provided by LED).

Exposure around 455 nm produces multitwinned seeds that reduce the surface energy as the most stable form of small AgNP seeds under these light conditions, which then grow into dodecahedra.¹³ However, 405, 627, and 720 nm excitation produces larger spheres, platelets, and rods respectively, which do not arise from seeds with twinning defects but are generally considered structures from single crystalline seeds.¹⁷ Therefore, it cannot be defects that direct the growth of nanoplates, rods, and larger spheres; it is rather the excitation wavelength and induced electromagnetic field that directs the growth. LEDs at 505 nm were also used to test the mechanism, and they produced particles with three major absorption bands at 541, 421, and 333 nm (SI and center cuvette in Figure 2). The absorption spectrum and SEM images correspond to a mixture of mostly hexagonal nanoplates and a small population of dodecahedra that have a similar major absorption at 541 nm, which helps confirm that the LEDs act as a “pull” to form particles with major absorption at or near the excitation wavelength. It is important to note that LEDs were preferred for excitation because of their high emission intensity and low cost. Other conditions required for LED transformation and experiments to support the aggregation/coalescence mechanism are stated in the SI.

In conclusion, we show a new photochemical synthesis of ~3 nm AgNPs used as seeds to photogenerate other nanostructures with size and morphology control, including larger spheres, as well as

dodecahedra, nanoplates, and nanorods. The size control and formation of nanorods are examples of a new method of synthesizing these structures, whereas dodecahedra and nanoplates provide evidence that the complex mixtures of stabilizing agents frequently used to photochemically produce these materials are unnecessary. The use of LEDs as excitation sources allows versatility and control in the cost-efficient manufacture of a variety of particles, which display predictable and controllable optical absorption over the entire visible range. Photochemically grown AgNP seeds are used to provide rapid and exceptional photochemical control over AgNP morphology and optical properties by exploiting the intense emission of light emitting diodes and the plasmon absorption of AgNPs.

Acknowledgment. We thank the Natural Sciences and Engineering Research Council for generous financial support, Michel Grenier who designed the LED exposure apparatus, and Dr. Yun Liu for her help with particle imaging.

Supporting Information Available: LED apparatus used to irradiate 3 mL samples in cuvettes, SEM images of AgNPs used to determine the average particle size after 405 nm irradiation, spectroscopic data from experiments attempting to convert seeds to plates and dodecahedra with a Xe lamp and band-pass filters, 590 nm LED irradiation results, spectra of seeds after ambient light exposure as well as experiments using a laser to attempt size control and PVA as a stabilizing agent are described. This material is available free of charge via the Internet at <http://pubs.acs.org>.

References

- (1) Kumar, C. *Metallic Nanomaterials*; Wiley: Weinheim, 2009; Vol. 1.
- (2) (a) Mitsudome, T.; Mikami, Y.; Mori, H.; Arita, S.; Mizugaki, T.; Jitsukawa, K.; Kaneda, K. *Chem. Commun.* **2009**, 3258. (b) Kelly, K. L.; Coronado, E.; Zhao, L. L.; Schatz, G. C. *J. Phys. Chem. B* **2003**, *107*, 668–677.
- (3) Sant’Ana, A. C.; Rocha, T. C. R.; Santos, P. S.; Zanchet, D.; Temperini, M. L. A. *J. Raman Spectrosc.* **2009**, *40*, 183–190.
- (4) Tiwari, V.; Oleg, T.; Darbha, G.; Hardy, W.; Singh, J.; Ray, P. *Chem. Phys. Lett.* **2007**, *446*, 77–82.
- (5) Shen, X. S.; Wang, G. Z.; Hong, X.; Xie, X.; Zhu, W.; Li, D. P. *J. Am. Chem. Soc.* **2009**, *131*, 10812–3.
- (6) (a) Alvarez-Puebla, R. A.; Aroca, R. F. *Anal. Chem.* **2009**, *81*, 2280–2285. (b) Caswell, K.; Bender, C.; Murphy, C. *Nano Lett.* **2003**, *3*, 667–669. (c) Metraux, G.; Mirkin, C. *Adv. Mater.* **2005**, *17*, 412–415. (d) Nam, K. T.; Lee, Y. J.; Krauland, E. M.; Kottmann, S. T.; Belcher, A. M. *ACS Nano* **2008**, *2*, 1480–6. (e) N’Gom, M.; Ringnalda, J.; Mansfield, J. F.; Agarwal, A.; Kotov, N.; Zaluzec, N. J.; Norris, T. B. *Nano Lett.* **2008**, *8*, 3200–3204. (f) Siekkinen, A.; McLellan, J.; Chen, J.; Xia, Y. *Chem. Phys. Lett.* **2006**, *432*, 491–496. (g) Sun, Y. G.; Mayers, B.; Herricks, T.; Xia, Y. N. *Nano Lett.* **2003**, *3*, 955–960. (h) Sun, Y. G.; Mayers, B.; Xia, Y. N. *Nano Lett.* **2003**, *3*, 675–679. (i) Chen, J.; Wiley, B.; Xia, Y. *Langmuir* **2007**, *23*, 4120–4129.
- (7) Aroca, R. *Surface-Enhanced Vibrational Spectroscopy*; Wiley: Chichester, 2006.
- (8) (a) Huang, H. H.; Ni, X. P.; Loy, G. L.; Chew, C. H.; Tan, K. L.; Loh, F. C.; Deng, J. F.; Xu, G. Q. *Langmuir* **1996**, *12*, 909–912. (b) Krylova, G. V.; Eremenko, A. M.; Smirnova, N. P.; Eustis, S. *Theor. Exp. Chem.* **2005**, *41*, 105–110. (c) Sakamoto, M.; Fujistuka, M.; Majima, T. *J. Photochem. Photobiol., C* **2009**, *10*, 33–56.
- (9) Pietroniro, B.; Kitaev, V. *Chem. Mater.* **2008**, *20*, 5186–5190.
- (10) (a) Jin, R. *Science* **2001**, *294*, 1901–1903. (b) Jin, R. C.; Cao, Y. C.; Hao, E. C.; Metraux, G. S.; Schatz, G. C.; Mirkin, C. A. *Nature* **2003**, *425*, 487–490. (c) Callegari, A.; Tonti, D.; Chergui, M. *Nano Lett.* **2003**, *3*, 1565–8.
- (11) Maier, S. A. *Plasmonics: Fundamentals and Applications*; Springer: New York, 2006.
- (12) Kreibitz, U.; Vollmer, M. *Optical Properties of Metal Clusters*; Springer, 1995; Vol. 25.
- (13) Zheng, X.; Zhao, X.; Guo, D.; Tang, B.; Xu, S.; Zhao, B.; Xu, W.; Lombardi, J. R. *Langmuir* **2009**, *25*, 3802–7.
- (14) Tanaka, Y.; Yoshikawa, H.; Itoh, T.; Ishikawa, M. *J. Phys. Chem. C* **2009**, *113*, 11856–11860.
- (15) Pal, A.; Pal, T. *J. Raman Spectrosc.* **1999**, *30*, 199–204.
- (16) Maillard, M.; Huang, P. R.; Brus, L. *Nano Lett.* **2003**, *3*, 1611–1615.
- (17) Tao, A. R.; Habas, S.; Yang, P. *Small* **2008**, *4*, 310–325.
- (18) Fujiwara, H.; Yanagida, S.; Kamat, P. V. *J. Phys. Chem. B* **1999**, *103*, 2589–2591.

JA910010B